Construction and Building Materials 143 (2017) 272–279

Contents lists available at ScienceDirect

Construction and Building Materials

journal homepage: www.elsevier.com/locate/conbuildmat

Comparison of long term performance between alkali activated slag and fly ash geopolymer concretes

Arie Wardhono [a], Chamila Gunasekara [b,*], David W. Law [b], Sujeeva Setunge [b]

[a] Department of Civil Engineering, State University of Surabaya (Universitas Negeri Surabaya), Kampus Unesa Ketintang, Surabaya 60231, Indonesia
[b] Civil and Infrastructure Engineering, School of Engineering, RMIT University, 124, La Trobe Street, Melbourne, Victoria 3000, Australia

HIGHLIGHTS

- Engineering properties of FAGP concrete improve from 28 to 540 days from casting.
- Continuing gel production of FAGP concrete densify microstrucre over time.
- Mechanical properties of AAS concrete decrease between 90 and 540 days from casting.
- Disjoining pressure & self-desiccation effect propagate cracks in AAS in long term.
- FAGP concrete is behaving in a similar manor to PC concrete.

ARTICLE INFO

Article history:
Received 29 December 2016
Received in revised form 1 March 2017
Accepted 14 March 2017

Keywords:
Fly ash geopolymer
Alkali activated slag
Mechanical properties
Durability
Long term performance

ABSTRACT

This paper reports the comparison of engineering properties of alkali activated slag (AAS) and low calcium fly ash geopolymer (FAGP) concretes up to 540 days. The results showed that the AAS concrete had higher compressive and tensile strength, elastic modulus and lower permeation characteristics than FAGP concrete in the initial 90 days. However, a reduction in AAS concrete performance was observed between 90 and 540 days, while an increase was noted in FAGP concrete over the same time period. The microscopy revealed that both reactions progressed beyond 90 days with the slag–alkali producing excess C–S–H gel which was observed to increase the crack propagation and crack width at latter ages, attributed to the combined effect of disjoining pressure and self-desiccation. The fly ash geopolymerization also continued following an initial 24 h heat curing resulting in a crack-free dense microstructure at 540 days. Overall the discrepancy in microstructural development beyond 90 days in the two concretes would explain the contradictory performance over the longer time frame.

1. Introduction

Concrete is the most widely used construction material in society today. Concrete is conventionally produced by using Portland cement (PC) as the primary binder with the ratio of PC in traditional concrete being approximately 10–15% by the mass of concrete. However, the production of PC has led to environmental concerns over the production of CO_2. Cement production has been estimated as contributing between 5 and 7% of the current anthropogenic CO_2 emissions worldwide [1,2], with the production of 1 ton of cement producing from 0.6 up to 1 ton of CO_2, depending on the power plant [3–5]. This had led to the adoption of waste materials, such as fly ash (FA) and ground granulated blast-furnace slag (GGBS), as a replacement for PC due to their ability to enhance the physical, chemical and mechanical properties of cements and concretes. More recently research has shown that it is possible to develop geopolymer concretes based solely on waste materials activated directly, without the presence of PC, utilizing an alkaline activator [6–12]. A major benefit of geopolymer concrete is that the reduction of CO_2 emission by 26–45% with the replacement of PC with no adverse economic effects [13–15].

In the geopolymerization process, alumina and silica species in FA rapidly react with highly alkaline activator solution and produce a three-dimensional polymeric chain and ring structure consisting of Si–O–Al–O bonds. The schematic formation of the final geopolymer product is sodium-aluminosilicate (N–A–S–H) gel, which governs the properties of low calcium fly ash geopolymer (FAGP) concrete [16]. Conversely, in AAS concrete, the calcium silicate hydrates (C–S–H) gel is the main resultant product of

* Corresponding author.
E-mail addresses: ariewardhono@unesa.ac.id (A. Wardhono), chamila.gunasekara@rmit.edu.au (C. Gunasekara), david.law@rmit.edu.au (D.W. Law), sujeeva.setunge@rmit.edu.au (S. Setunge).

http://dx.doi.org/10.1016/j.conbuildmat.2017.03.153
0950-0618/

geopolymerisation, which is similar to the primary binding phase of PC and blended cement concretes [17].

Hardjito & Rangan [18] and Fernandez-Jimenez et al. [19] studied the mechanical properties of FAGP concrete up to 90 days and observed that it has a comparable compressive strength, higher flexural and splitting tensile strength, but a lower elastic modulus to that of PC concrete. Ryu et al. [20] showed that the splitting tensile strength to compressive strength ratio at 28 days ranged between 7.8 and 8.2%, similar to that of PC concrete. Neupane et al. [21] and Loya et al. [22] also found that the relationship between elastic modulus and compressive strength of FAGP concrete is similar to that of PC concrete. Research has also demonstrated similar mechanical properties for AAS concrete to PC concrete for periods up to 90 day [17,23,24], though a reduction of compressive strength with time has been reported by Collins and Sanjayan [25], while Bernal et al. [23] found that AAS concrete has a comparable compressive strength, but higher flexural strength than PC concrete.

Considering the permeation characteristics, Bernal et al. [26] showed that the binder content of the concretes has a particularly strong effect on the water absorption properties of AAS concrete. Collins and Sanjayan [27] reported that AAS concrete has a lower water absorption due to the presence of very refined, tortuous and closed porosity in the concrete. Moreover, Olivia et al. [28] stated that fly ash geopolymer concrete exhibits low water absorption and sorptivity compared to the PC concrete. The water/binder ratio and well-graded aggregate influence were noted to influence the permeation characteristics. However, these studies were only conducted up to 90 days, and there is no comparison between AAS and fly ash geopolymer concretes over the long term.

In order to function as a construction material, it is imperative that both AAS and FAGP concretes maintain their performance over the design life of a structure. This paper reports the details of an experimental research program that has been undertaken to investigate a range of mechanical and durability properties of AAS and FAGP concrete up to 540 days. The properties assessed were compressive strength, flexural and splitting tensile strength, elastic modulus, water absorption and water permeability.

2. Significance of research

Published research to date on AAS and FAGP concrete has been reported their performance only up to 90 days (short term), in each study using a mixing process unique to that study, with no comparison of long term performance between them. This research reports the performance of AAS and FAGP concretes up to one and half year while applying the same mixing process, providing a systematic long term comparison study of the engineering properties between them. Research data presented here thus will be extremely useful to comprehend the long term behavior of AAS and FAGP concretes.

3. Experimental procedure

3.1. Materials used

The GGBS was a construction grade slag conforming to Australian Standard, AS 3582.2 [29], with the basicity coefficient of 0.81 and the hydration modulus of 1.5. The low calcium, class F FA conforming to Australian standard, AS 3582.1 [30] was obtained from Tarong power station in Australia. The chemical composition, particle size distribution and mineralogical composition of fly ash and GGBS, determined by X-ray fluorescence (XRF), Malvern particle size analyzer instruments and X-ray diffraction (XRD), respectively are shown in Table 1 and 2. Brunauer Emmett Teller (BET) method by N_2 absorption was used to determine the fly ash surface area.

The alkaline activator used in AAS and FAGP concretes consisted of a mixture of Commercially available sodium silicate solution with a specific gravity of 1.53 and an alkaline modulus ratio (Ms) equal to 2 (where Ms = SiO_2/Na_2O, Na_2O = 14.7%, SiO_2 = 29.4% and 55.9% H_2O by mass), and sodium hydroxide solution. A 15 M NaOH solution was used for the manufacture of the FAGP and a 10 M NaOH solution used for the AAS. The selection of two different molarity in sodium hydroxide solution is dependent on the mix optimization based on 28-day compressive strength Both coarse and fine aggregate were prepared in accordance with AS 1141.5 [31]. The aggregate was in a saturated surface dry condition. The fine aggregate was river sand in uncrushed form with a specific gravity of 2.5 and a fineness modulus of 3.0. The coarse aggregate was crushed granite aggregate of two-grain sizes: 7 mm, 2.58 specific gravity and 1.60% water absorption, and 10 mm, 2.62 specific gravity and 0.74% water absorption. Demineralized water was used throughout the experiment.

3.2. Mix proportions and specimen preparations

Mix proportions used in AAS and FAGP concretes were based on a previous study, which is summarized in Table 3 [32]. The activator modulus (SiO_2/Na_2O in alkaline activator) is fixed at 1.0 for both concretes while Na_2O dosage (Na_2O in alkaline activator/FA) is fixed at 5% and 15% in the AAS and FAGP concretes, respectively. The ratio of components, such as binder (GGBS or FA), alkaline activator, aggregate and water, was calculated based on the absolute volume method [33]. The total aggregate in the concrete was kept to 64% of the entire mixture by volume for all mixes. A water solid ratio (w/s) of 0.44 and 0.37 was used to prepare the AAS and FAGP concrete, which gave a consistent workability in the mixing process. The total liquid and solid content is shown in Table 3. The mass of water in the mix was taken as the sum of mass of water contained in the sodium silicate, sodium hydroxide and added water. The mass of solid is taken as the sum of binder (GGBS or FA), the solids in the sodium silicate and the sodium hydroxide solution.

The mixing of concretes was carried out using a 120 liter concrete mixer. The dry materials (GGBS or FA, fine aggregates and coarse aggregates) were mixed first for 4 min. Then activator and water were added to the dry mix and mixed continuously for another 8 min until the mixture was glossy and well combined. The mixture was then poured into moulds and vibrated using a vibration table for 1 min to remove air bubbles. After vibration both AAS and FAGP concrete specimens were kept at room temperature (23 °C) for 1 day. The AAS specimens were demoulded, water-cured (23 °C) for 6 days and kept at room temperature until being tested. The FAGP specimens were heat-cured (80 °C) using dry oven for 24 h, the moulds were removed from the oven and left to cool to room temperature before demoulding, and the samples were kept at room temperature until being tested.

3.3. Testing

The compressive strength test was performed by MTS machine with a loading rate of 20 MPa/min according to AS 1012.9 [34]. The flexural and splitting tensile strength tests were conducted to determine the tensile strength of concretes in accordance with AS 1012.11 [35] and AS 1012.10 [36] respectively. The flexural tensile strength test was carried out on a MTS machine with additional testing apparatus under a four point bending test with a loading rate of 1 MPa/min. The splitting tensile strength test was performed on MTS machine equipped with splitting tensile strength test equipment under a loading rate of 1.5 MPa/min. The elastic modulus was determined using Tecnotest concrete testing machine coupled with the compressometer/extensometer with a loading rate of 0.25 MPa/s in accordance with AS 1012.17 [37], and dry density was measured accordance with AS 1012.12.2 [38].

The ultrasonic pulse velocity test was conducted in accordance with ASTM C597 standard [39] using a portable ultrasonic non-destructive digital indicating tester with a 54 kHz transducer. The water permeability tests were performed using the Autoclam Permeability System. Water is admitted into the test area through a priming pump and the pressure inside is increased to 0.5 bar at the end of the priming. The quantity of water flowing into the concrete is recorded every minute for duration of 15 min. The water absorption test was carried out in accordance with AS 1012.21 [40] standard to determine the immersed absorption. Immersed absorption (*Ai*) is the ratio (%) of the mass of water contained in a concrete specimen, and was used to determine the water absorption of concrete specimens. The apparent volume of permeable void (AVPV) percentage is also measured in accordance with AS 1012.21 standard [40]. The specimens of 100 mm diameter × 200 mm long cylinders were cut into four equal slices for both experiments and the result reported is the average of the results for the four slices. All tests were conducted at 28, 56, 90, 180, 360 and 540 days of casting. The reported test results in each specific test for each concrete are an average of three samples.

The microstructure development was observed using scanning electron microscopy (SEM) imaging employing backscatter electron detector with 15 eV of energy. Energy dispersive X-ray spectroscopy (EDS) analysis was performed using Oxford instruments nano-analysis software (AZtec 2.1) to determine the chemical composition of the reacted geopolymer. Specimens were cut using a diamond saw to a size of 2–4 mm in height and 5–10 mm in diameter. The samples were subsequently carbon coated and then mounted on the SEM sample stage with conductive, double-sided carbon tape. A total of three samples were investigated for each geopolymer concrete.

Table 1
Chemical composition.

Material	By weight (%)											Loss on Ignition (%)
	SiO_2	Al_2O_3	Fe_2O_3	CaO	P_2O_5	TiO_2	MgO	K_2O	SO_3	MnO	Na_2O	
GGBS	36.9	14.2	0.3	36.0	0.4	0.6	5.1	0.1	6.1	0.4	0	0.3
FA	70.3	23.1	1.4	0.2	0.2	2.6	0.6	0.9	0.2	0	0.4	2.0

Table 2
Physical and mineralogical properties.

Properties investigated		GGBS	FA
Specific Gravity		2.85	2.12
BET Surface Area, (m^2/kg)		3852	1876
Fineness (%)	at 5 μm	20.9	22.7
	at 10 μm	43.5	43.0
	at 20 μm	71.9	63.0
	at 45 μm	96.9	81.8
	at 75 μm	100.0	91.2
Amorphous content (%)		71.7	66.3
Crystalline content (%)		28.3	33.7

4. Experimental results

4.1. Mechanical properties

4.1.1. Density and compressive strength

The dry density and compressive strength development of AAS and FAGP concretes between 28 and 540 days are displayed in Fig. 1(a and b). The dry density of AAS and FAGP concretes ranged between 2453–2460 and 2302–2326 kg/m^3, respectively from 28 to 540 days. While the density of FAGP concrete is slightly lower than PC concrete, which is characteristically cited as 2400 kg/m^3 [41], the AAS concrete was marginally higher compared to PC concrete. It is noted that both concretes dsplay a less than 1% of densitly increase during the 28 and 540 days period.

The AAS concrete had a higher compressive strength than FAGP concrete throughout. The AAS achieved 39.5 MPa at 28 days, compared to an initial strength of 22.4 MPa for the FAGP. However, the FAGP concrete gave an increase in strength with time, achieving 33.2 MPa after 360 days, which then remains constant to 540 days. However, while the AAS concrete does display an increase in strength to 41.6 MPa at 56 days no further increase is observed. Indeed a slight reduction in strength is noted, 40.2 MPa at 180 days, though a strength above 40 MPa is maintained throughout the remaining period. Overall, whilst FAGP concrete displayed a 48.2% (10.2 MPa) compressive strength increase from 28 to 540 days, only a 2.3% (0.9 MPa) strength development is observed for the AAS concrete in same period. This indicates an ongoing geopolymerisation reaction in FAGP concrete following the initial heat curing [42,43], while the same is not observed for the AAS.

4.1.2. Tensile strength

The flexural strength and splitting tensile strength development of AAS and FAGP concretes between 28 and 540 days are shown in Fig. 2(a and b). Similar to compressive strength development, the flexural strength of FAGP concrete tended to increase with time. It ranged from 4.7 to 7.2 MPa between 28 and 365 days, i.e. a 53.2% of flexural strength increase during this period. The AAS achieves a 6 MPa flexural strength at 28 days, compared to an initial flexural strength of 4.7 MPa for the FAGP. However, the AAS concrete shows a decrease in flexural strength with time, achieving 5.2 MPa at 540 days, which is a 13.3% fall in strength. It is noted that both FAGP and AAS concretes obtained similar flexural strength (5.8 MPa) at 90 days. Subsequently, FAGP increased in flexural strength, while AAS decreased, during the 90–540 day period. Overall the flexural strength of the FAGP and AAS concrete ranged between 20–22% and 14–16% of the compressive strength respectively, compared to a range of 9–12% typically cited for PC concrete [11,24].

On the other hand, both AAS and FAGP concretes show a lower splitting tensile strength than corresponding flexural strengths as shown in Fig. 2. The splitting tensile strength of FGAP concrete increased with time, from 2.1 to 4.1 MPa between 28 and 540 days, and varied from 9 to 12% of the compressive strength. The AAS showed higher splitting tensile strength than FAGP concrete up to 90 days, but after that FAGP showed a significant improvement compared to the AAS concrete and achieved a 24.2% increase in splitting tensile strength at 540 days.

4.1.3. Elastic modulus

The modulus of elasticity development of AAS and FAGP concretes between 28 and 540 days are shown in Fig. 3. This property of concrete expresses the ratio between a certain range of unit stress and unit elongation within the elastic limit. A higher elastic modulus will represent a better quality of concrete specimen. The elastic modulus of FAGP and AAS concretes ranged between 8022–15942 and 26768–15279 MPa, respectively over the 28 to 540 day period. The AAS achieves a significantly high elastic modulus (26768 MPa) at 28 days, compared to an initial elastic modulus of 8022 MPa for the FAGP concrete. It is worth noting that the data again shows contrasting trends, with the FAGP concrete displaying an increase with time, while the AAS concrete shows a decrease with time, such that by 540 days the FAGP has a higher elastic modulus than the AAS concrete. The FAGP concrete has a twofold increase of elastic modulus from 28 to 540 days, but AAS concrete shows a 43% decrease during this time interval.

4.2. Permeation properties

4.2.1. Water absorption and AVPV

The water absorption and AVPV of AAS and FAGP concretes are shown in Fig. 4(a and b). The FAGP concrete had higher water absorption (7.75%) than AAS concrete (4.79%) at 28 days. However, the long term data displays a reduction of water absorption in FAGP to 6.82% at 360 days and to 6.74% at 540 days with an overall decrease of 13% observed from 28 to 540 days. In PC concrete, a water absorption greater than 5% is classified as high permeable concrete, while less than 3% is classified as low permeable concrete [44]. The FAGP concrete exceeded this upper limit at all ages and behaved as high permeable concrete, which indicates a highly porous external surface. The AAS concrete shows water absorption less than 5% in the first 90 days, but then exceeded this upper limit achieving 5.36% at 540 days. These trends are consistent with those observed for the flexural strength and elastic modulus, indicating an improvement in density of the pore-structure for the FAGP over the longer term, while also suggesting a reduction in density within the pore-structure for the AAS concrete during this period.

The AVPV is a percentage of pore space such as capillary pores, gel pores and air voids within the concrete. The trends observed were similar to water absorption for both concretes, AVPV decreasing with time in FAGP, while AAS increases. In PC concrete an AVPV less than 13% is classified as good quality concrete, while greater than 18% is classified as poor quality concrete [45]. It is noted that AAS concrete at all ages were below this lower limit though it has an increase of AVPV with time, indicating limited pore interconnectivity in their pore-structure. However, the FAGP concrete had AVPV percentage between 13% and 15% at all ages.

4.2.2. Water permeability & UPV

The variation of water permeability index with time is shown in Fig. 5. In the water permeability test, both capillary absorption and the applied pressure contribute to the rate of water flow. The slope of the linear regression curve between water flow and square root of time provides the corresponding water permeability index [46], given in Fig. 6. The AAS concrete showed an increase of water permeability index with age, but is classified as low water permeable concrete at all ages as the WPI did not exceed 1.3×10^{-7} $m^3/\sqrt{min}$ [47]. The FAGP concrete had a signif-

Table 3
Mix design details (kg/m^3).

Concrete	GGBS (kg)	FA (kg)	Aggregates (kg)			Alkali Activator (kg)				Added Water (kg)	Total Water (kg)	Total Solid (kg)
			Sand	7 mm	10 mm	Na_2SiO_3 (Water)	Na_2SiO_3 (Solid)	NaOH (Water)	NaOH (Solid)			
AAS	415	–	784	346	693	40	31	29	17	136	205	463
FAGP	–	409	686	303	606	114	90	80	49	10	204	548

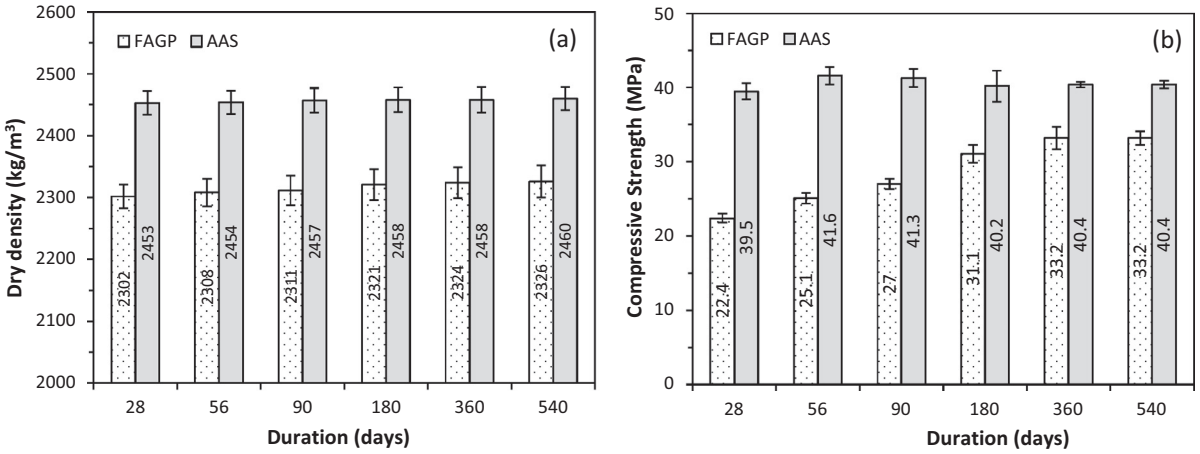

Fig. 1. (a) Density and (b) Compressive strength development vs time.

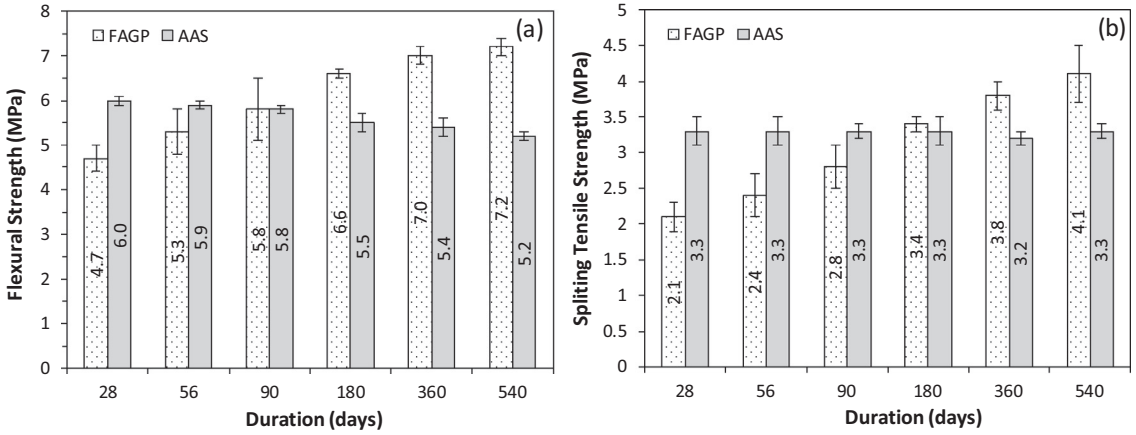

Fig. 2. (a) Flexural strength and (b) Splitting tensile strength development vs time.

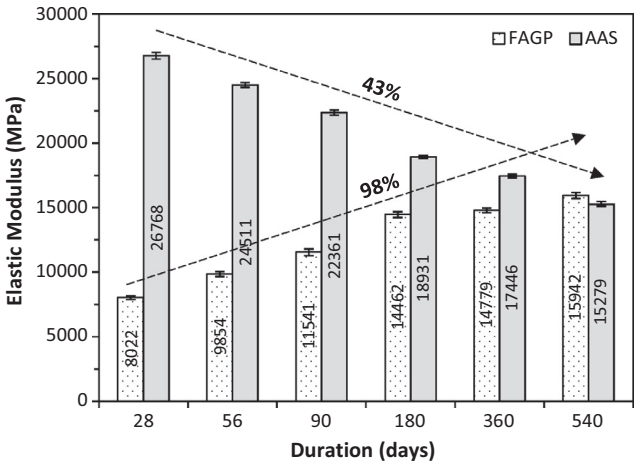

Fig. 3. Elastic modulus development vs time.

icantly higher water permeability index than AAS up to 90 days and was well above the minimum limit of low water permeable concrete [47]. However, it dramatically decreased by 180 days and further reduced at later ages, having a lower value than AAS concrete at 360 and 540 days. This is again consistent with on-going geopolymerization and in agreement with the corresponding UPV and strength data.

Fig. 6 shows the ultrasonic pulse velocity (UPV) changes with the age of AAS and FAGP concrete. Generally, the pulse velocity values represents the uniformity and the presence of defects in the microstructure and pore-structure, such as voids and cracks [48], which directly influence to the permeation properties of concrete. The FAGP concrete displays an increase of UPV with age while AAS has a fall from 3.91 to 3.62 between 28 and 540 days. The standard pulse velocity of PC concrete generally falls in the range 3.5 to 4.5 km/s [49], which can be categorized as being in good condition which implies that the concrete is free from any large voids or cracks that may affect the long term structural reliability. It is interesting to note that while AAS shows a decrease of UPV with time, all the data points are well above the 3.5 km/s. The FAGP concrete is identified as poor quality concrete with UPV values below 3 km/s [50] at 56 days, however it obtained a value of 3.5 km/s of UPV by 540 days.

Overall the data from the permeability properties would further suggest ongoing geopolymerization and concurrent gel formation resulting in a denser microstructure and pore-structure for FAGP concrete over the 540 days. However, the permeation properties would suggest that there is no improvement in the AAS concrete beyond 90 days, with even a slight deterioration observed.

5. Discussion

5.1. Microstrucre

The microstructural development of FAGP concrete at 28, 56, 90, 180, 360 and 540 days is displayed in the SEM images in Fig. 7. A non-uniform, heterogeneous aluminosilicate gel matrix with a numbers of unreacted/partially reacted FA particles was observed in the microstructure at 28 and 56 days. This was comprised of unreacted fly ash particles that were separated from the geopolymeric binder, indicating weak adhesion between the gel and the particles. In addition there were also partially dissolved particles embedded in the precipitated gel. The unreacted/partially

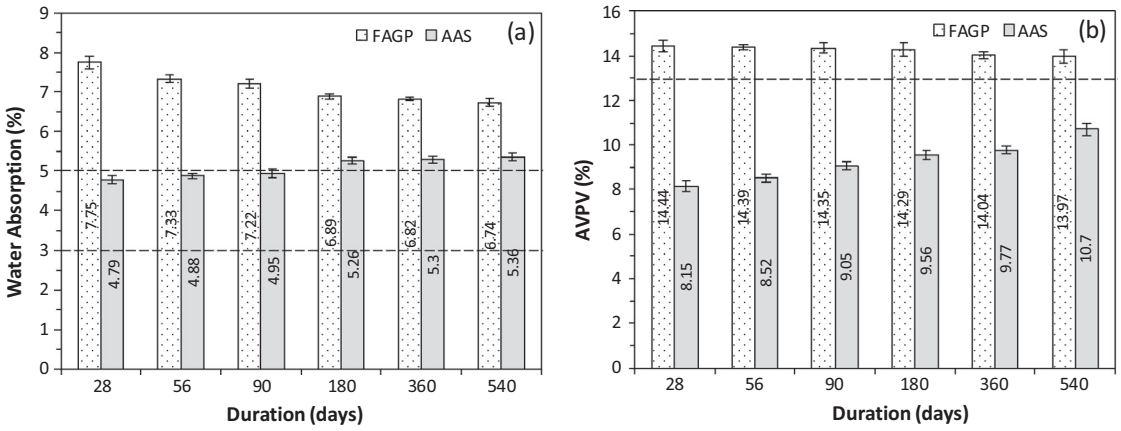

Fig. 4. (a) Water absorption and (b) AVPV vs. time.

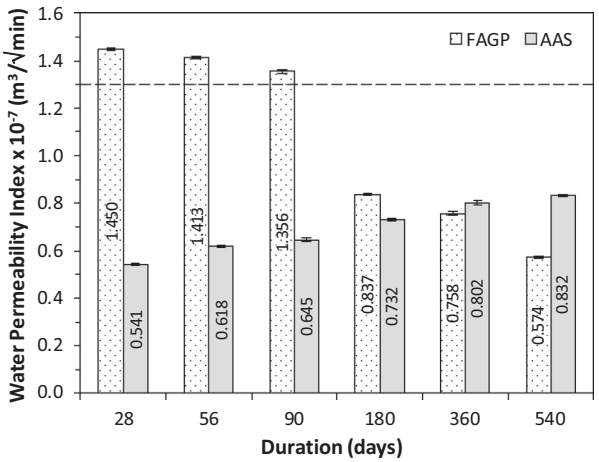

Fig. 5. Water permeability index vs time.

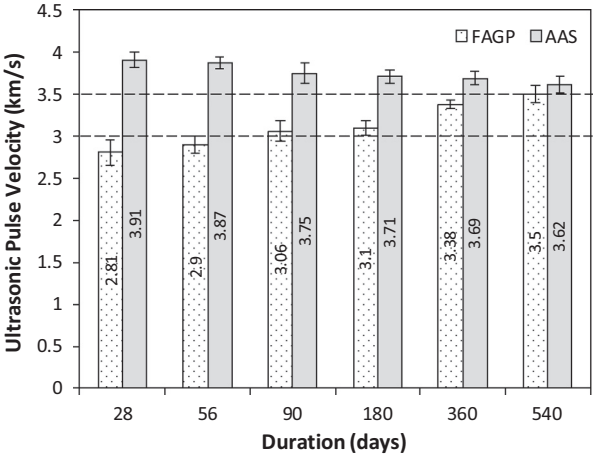

Fig. 6. Ultrasonic pulse velocity vs time.

reacted FA particles behave as composites. These composites and the interface between them and the geopolymer matrix is hypothesized as an area of weakness and thus has a significant bearing on the overall strength of the concrete [51]. Moreover micro cracks were distributed throughout the gel matrix. It was noted that more cracks and greater crack widths were observed in the 28 and 56 day specimens compared to those at latter ages. The occurrence of these micro cracks was most likely due to evaporation of the water and self-desiccation during the heat curing stage. Furthermore, the raw FA contains 2% unburnt carbon, Table 1. The unburnt carbon acts as an inert particulate in the gel matrix, which can support the crack propagation. It is hypothesized that a combination of the unreacted FA particles coupled with the presence of the micro cracks resulted in the initial lower compressive strength of FAGP.

It is understood that the Si/Al (atomic) ratio determines the structure of the geopolymer backbone [52,53]. In this study, Si/Al ratio of FAGP concrete ranged between 4.27 and 3.41 over the 28–540 days period. As such, the geopolymer structure was inferred to be polysialate–disiloxo (Si–O–Al–O–Si–O–Si–O). In FAGP concrete, the Si/Al ratio decreased with age indicating an on-going geopolymerization process beyond the 90 day time period, with continuous gel formation along with incorporation of alumina into the silicate backbone.

The FAGP microstructure shows a decrease in the number of unreacted particles at 360 and 540 days, further substantiating the indication that there has been some additional geopolymerization and gel formation. The SEM indicated the gel had diffused through the surface covering and coalescing the remaining partially reacted FA spheres together. The gel was also observed to fill the interior voids, resulting in the formation of a semi-homogeneous, but highly compacted dense microstructure at 540 days.

The decrease in the Si/Al ratio coupled with this semi-homogeneous and compact microstructure observed is hypothesized as the reason that the FAGP had a significantly improved performance at a later age, compared to the initial 90 days period.

The microstructural development of AAS concrete is displayed in Fig. 8. A fairly uniform, but heterogeneous gel matrix can be seen at 28 days. Most of the slag grains have been partially dissolved by the alkali solution, forming a C-S-H gel with the silica from the activator solution. Moreover, several small micro cracks had been formed on the surface of the unreacted/partially reacted slag grains. This is attributed to a rapid reaction between slag and alkaline activator in the initial period [23,25]. The microstructural development observed shows that in the period from 28 to 90 days additional C-S-H gel, due to the dissolution of remaining unreacted/partially reacted slag grains, with significantly less unreacted/partially reacted grains being observed at 90 days. This resulted in formation of densely packed microstrucre at 90 days. Whilst this matrix contains fewer micro cracks compared to those observed at 28 days, the width of the cracks at the interface of C-S-H gel and partially reacted slag particles is wider. The formation of micro-cracks at the slag grain/aggregate interface has also been reported by Collins and Sanjayan [25].

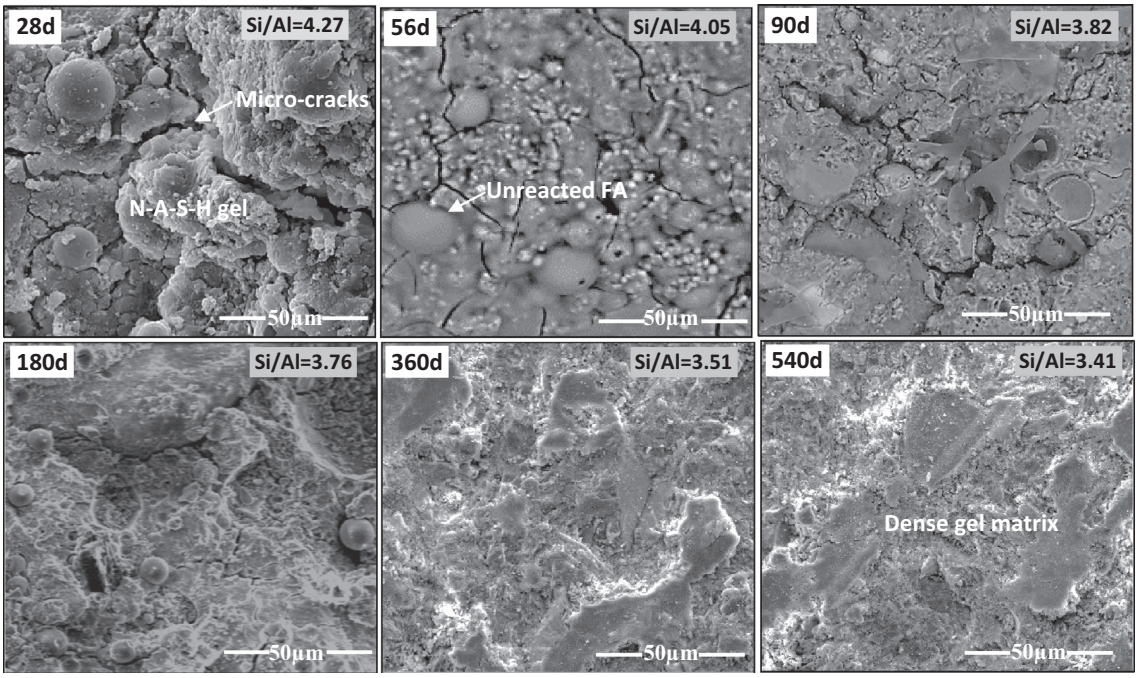

Fig. 7. Microstructural development of FAGP concrete.

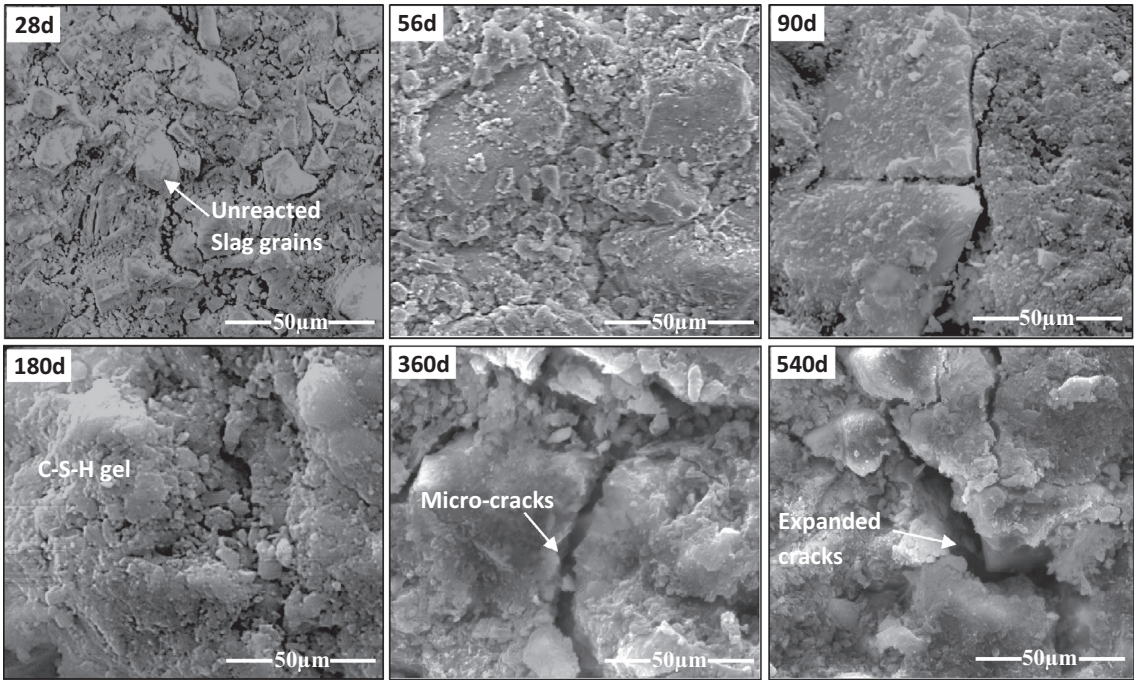

Fig. 8. Microstructural development of AAS concrete.

It is noted that there is a significant discrepancy of AAS microstructure before and after 90 days. The uniformity and density of the gel matrix drastically reduced between 90 and 180 days, and a less compacted, loosely packed gel matrix was formed at 180 days. It is hypothesized that as the reaction continued it produces additional C-S-H gel which led to the formation of wider cracks at 180 days. These cracks were seen to further increase at 360 and 540 days. This is attributed to the combined effect of disjoining pressure and the self-desiccation effect. This resulted in formation of less dense small gel units, as observed at 360 and 540, days rather than an interconnected dense gel matrix, as produced in the initial 90 days.

Data demonstrated in this study is consistent with those reported by literature [19,20,54] up to first 90 days. This improvement continues in similar manner up to 540 days. In contrast, the AAS concrete shows better initial performance than FAGP concrete, with some increase in performance, other than elastic modulus, up to 90 days, which is in agreement with literature [23,32]. However, it is noted that over the longer term data (360 and 540 days) the AAS concrete shows a reduction in engineering properties, which

commenced post 90 days. The contradictory behaviour is reflected in the changes observed in their microstructure between 90 and 540 days, Figs. 7 and 8.

5.2. Tensile strength and elastic modulus

The tensile strength (i.e. flexural and splitting strength) of FAGP and AAS concrete is strongly dependent on the gel-aggregate bond strength. The gel-aggregate zone is critical because it is known to have a different microstructure from the bulk of hardened gel paste and the interface is also considered as the specific location of early cracking. This is primarily caused by incomplete packing of unreacted fly ash/slag grains in the transition between the gel paste and coarse aggregates as the gel formation is strongly dependent on the degree of alkali reactivity of fly ash/slag particles. In this study, both fly ash and slag contain approximately similar amorphous content, Table 2, which is an important factor for alkali dissolution and gel precipitation [55,56]. However, recent research [54,57,58] has shown that it is not only the total amorphous content but also the distribution of this in the fly ash/slag grains that influences the dissolution process and variances in microstructure formation. On the other hand, the elastic modulus of FAGP and AAS concrete is affected by the modulus of aggregate and gel paste. FAGP concrete had a less compacted heterogeneous microstructure up to 90 days. However, beyond 90 days the microstructure was significantly denser, consistent with continuing dissolution and gel formation increasing the physical solidity. The improvement in the gel-microstructure, as well the gel-aggregate interfacial zone is hypothesized as the reason for the observed improved elastic modulus and tensile strength development in FAGP concrete between 28 and 540 days. Conversely, the AAS concrete had a dense gel matrix with less micro cracks in the first 90 days, but these were observed to increase over time. This propagation of the cracks and the associated reduction of packing density of the gel matrix is hypothesized as the cause the lack of development in the compressive and tensile strength, as well the significant fall of elastic modulus over time.

5.3. Transport properties

The reaction products and the packing density are crucial in determining the water absorption. Water absorption is primarily governed by the capillary suction. Capillary suction is governed by the connectivity of the concrete surface to the bulk concrete via the pores in the gel paste. The FAGP concrete however displayed a high AVPV percentage, which is also dependent on the interconnectivity of the capillaries in the concrete. The FAGP concrete also displayed high water permeability characteristics at 90 days, but it significantly reduced with time and behaved as low permeable concrete at 360 and 540 days. In the water permeability test, the applied pressure is the principal driver of water ingress rather than capillary suction, and this would give an indication about the overall image of pore-structure throughout the concrete specimen. This reduction in water permeability with time is attributed to the development of sodium-aluminosilicate gel during the on-going geopolymerisation process. The additional gel fills the interface between the geopolymer pastes and the aggregates, and reduces the volume of the pore-structure leading to a denser the microstructure, as reflected in the increase of UPV values over time.

It is noted that AAS concrete had lower permeation characteristics than FAGP up to 90 days. However, a considerable increase of water absorption, interconnectivity of pore-structure and water permeability in AAS concrete is observed after 90 days, which correlates with its microstructural changes. The increase in crack widths observed in the gel matrix, Fig. 8, would lead to an increase in the permeation characteristics at later ages.

5.4. Comparison

The overall trends observed for the mechanical and permeation properties show that the FAGP concrete is behaving in a similar manor to PC concrete, where the engineering properties improve with time. The AAS concrete, however, does not follow these trends with no increase in performance beyond 90 days, and a slight decrease actually observed in a number of these properties. In addition to the mechanical properties the long term durability of AAS and FAGP concrete is dependent upon the permeability characteristics of concrete which is associated with the ability of the surface layer to resist the penetration of water, carbon dioxide and water-borne chlorides into the concrete and initiate reinforcement corrosion. The rate of this is a function of the packing density of C-S-H/aluminosilicate gel matrix, the porosity and the connectivity of the pore structure. The data obtained up to 540 days suggests that FAGP concrete improves resistance to water permeation with age due to on-going geopolymerization and give a performance comparable with PC and blended cement concretes. Thus while the AAS concrete shows significantly greater compressive, tensile and flexural strength, coupled with a higher modulus of elasticity and lower water absorption, AVPV and water permeability in the initial 90 days and while the overall performance compared with similar strength PC concrete remains good, by 540 days only the compressive strength remains above the FAGP concrete, and the water absorption and AVPV lower, with the modulus of elasticity similar and the flexural strength less and the water permeability higher than that of the FAGP.

6. Summary and conclusions

The compressive strength, flexural strength, splitting tensile strength, elastic modulus, water absorption, pore-interconnectivity and water permeability for AAS and FAGP concretes were studied experimentally up to 540 days. The principal conclusions from the work presented are:

- Compressive strength of FAGP and AAS concretes ranged between 22.2–33.2 MPa and 39.5–40.4 MPa from 28 to 540 days, respectively. The order of ~48% and ~2% strength increase is observed in two concretes, respectively during this period.
- FAGP concrete showed ~53% flexural strength increase between 28 and 540 days, compared to the ~13% decrease in AAS concrete. Moreover, FAGP concrete achieved a twofold splitting tensile strength evolution during this time while AAS remained constant throughout.
- AAS showed significantly higher early stiffness (i.e. elastic modulus) than FAGP concrete in the first 90 days. However, the elastic modulus of AAS concrete drastically reduced with time and displayed ~43% drop from 28 to 540 days, opposed to that of FAGP which had a ~98% increase in the same period.
- FAGP concrete had a higher water permeability index than AAS in the first 90 days, but significantly reduced with the age. The water permeability of the AAS increased with time, but was classified as low permeable concrete over the entire testing period.
- The combined effect of disjoining pressure and self-desiccation due to the on-going reaction and C–S–H gel formation causing the propagation of wider cracks in microstructure, is hypothesized as the reason for the reduction in engineering performance observed for the AAS concrete over the long term.

- The increase of in the packing density of the aluminosilicate gel matrix is hypothesized as positively influencing the elastic modulus and strength development in FAGP concrete observed between 90 and 540 days.

Acknowledgments

Materials support from the Independence Cement Pty. Ltd. Australia and PQ Australia for carrying out this research project is gratefully acknowledged. The authors also wish to acknowledge the X-ray facility and Microscopy & Microanalysis facility provided by RMIT University and the scientific and technical assistance.

References

[1] C. Meyer, The greening of the concrete industry, Cement Concr. Compos. 31 (8) (2009) 601–605.
[2] C. Chen et al., Environmental impact of cement production: detail of the different processes and cement plant variability evaluation, J. Cleaner Prod. 18 (5) (2010) 478–485.
[3] J. Peng et al., Modeling of carbon dioxide measurement on cement plants, Adv. Mater. Res. 610–613 (1) (2013) 2120–2128.
[4] C. Li et al., CO2 emissions due to cement manufacture, Mater. Sci. Forum 685 (1) (2011) 181–187.
[5] D.N. Huntzinger, T.D. Eatmon, A life-cycle assessment of Portland cement manufacturing: comparing the traditional process with alternative technologies, J. Cleaner Prod. 17 (7) (2009) 668–675.
[6] W.D.A. Rickard, G.J.G. Gluth, K. Pistol, In situ thermo-mechanical testing of fly ash geopolymer concretes made with quartz and expanded clay aggregates, Cem. Concr. Res. 80 (2016) 33–43.
[7] B. Singh et al., Geopolymer concrete: a review of some recent developments, Constr. Build. Mater. 85 (2015) 78–90.
[8] J.L. Provis, Geopolymers and other alkali activated materials: why, how, and what?, Mater Struct. 47 (1–2) (2014) 11–25.
[9] P. Chindaprasirt, W. Chalee, Effect of sodium hydroxide concentration on chloride penetration and steel corrosion of fly ash-based geopolymer concrete under marine site, Constr. Build. Mater. 63 (1) (2014) 303–310.
[10] M. Soutsos et al., Factors influencing the compressive strength of fly ash based geopolymers, Constr. Build. Mater. 110 (1) (2016) 355–368.
[11] P. Chindaprasirt et al., Controlling ettringite formation in FBC fly ash geopolymer concrete, Cement Concr. Compos. 41 (2013) 24–28.
[12] A. Cwirzen et al., Effects of curing: comparison of optimised alkali-activated PC-FA-BFS and PC concretes, Mag. Concr. Res. 66 (6) (2014) 315–323.
[13] B.C. McLellan et al., Costs and carbon emissions for geopolymer pastes in comparison to ordinary portland cement, J. Cleaner Prod. 19 (9) (2011) 1080–1090.
[14] G. Habert, J.B. d'Espinose de Lacaillerie, and N. Roussel, *An environmental evaluation of geopolymer based concrete production: reviewing current research trends*, J. Cleaner Prod. 19 (11) (2011) 1229–1238.
[15] T. Stengel, J. Reger, D. Heinz, LCA of geopolymer concrete - what is the environmental benefit?, Proceedings of the 24th biennial conference of the Concrete Institute of Australia 2009. Sydney, Australia, 2009.
[16] J. Davidovits, Geopolymer chemistry and sustainable development. The poly (sialate) terminology: a very useful and simple model for the promotion and understanding of green-chemistry, in: Proceedings of 2005 geopolymer conference, 2005.
[17] A.R. Sakulich et al., Mechanical and microstructural characterization of an alkali-activated slag/limestone fine aggregate concrete, Constr. Build. Mater. 23 (8) (2009) 2951–2957.
[18] D. Hardjito, B.V. Rangan, Development and properties of low-calcium fly ash-based geopolymer concrete, in: Research Report-GC1, Curtin University of Technology, Perth, Australia, 2005, pp. 1–103.
[19] A. Fernández-Jiménez, A. Palomo, L.-H. Cecilio, Engineering properties of alkali-activated fly ash concrete, ACI Mater. J. 103 (2) (2006) 106–112.
[20] G.S. Ryu et al., The mechanical properties of fly ash-based geopolymer concrete with alkaline activators, Constr. Build. Mater. 47 (1) (2013) 409–418.
[21] K. Neupane et al., Mechanical properties of Geopolymer concrete: applicability of relationships defined by AS 3600, Concr. Australia 40 (1) (2014) 50–56.
[22] E.I. Diaz-Loya, E.N. Allouche, S. Vaidya, Mechanical properties of fly-ash-based geopolymer concrete, ACI Mater. J. 108 (3) (2011) 300–306.
[23] S.A. Bernal, R.M. de Gutiérrez, J.L. Provis, Engineering and durability properties of concretes based on alkali-activated granulated blast furnace slag/metakaolin blends, Constr. Build. Mater. 33 (1) (2012) 99–108.
[24] D. Bondar et al., Engineering properties of alkali-activated natural pozzolan concrete, ACI Mater. J. 108 (1) (2011) 64–72.
[25] F. Collins, J. Sanjayan, Microcracking and strength development of alkali activated slag concrete, Cement Concr. Compos. 23 (4) (2001) 345–352.
[26] S.A. Bernal et al., Effect of binder content on the performance of alkali-activated slag concretes, Cem. Concr. Res. 41 (1) (2011) 1–8.
[27] F. Collins, J. Sanjayan, Effect of pore size distribution on drying shrinking of alkali-activated slag concrete, Cem. Concr. Res. 30 (9) (2000) 1401–1406.
[28] M. Olivia, P. Sarker, H. Nikraz, Water penetrability of low calcium fly ash geopolymer concrete, Proc. ICCBT2008-A, vol. 46, 2008, pp. 517–530.
[29] AS, Supplementary cementitious materials – Slag – Ground granulated blast-furnace, in: AS (Australian Standards), Standards Australia, Australia, 2016, pp. 1–16.
[30] AS, Supplementary cementitious materials for use with portland and blended cement, Part 1: Fly ash, in: AS (Australian Standards), Standards Australia, Australia, 1998, pp. 1–13.
[31] AS, Methods for sampling and testing aggregates, Method 5: Particle density and water absorption of fine aggregate, in: AS (Australian Standards), Standards Australia, Australia, 2000, pp. 1–8.
[32] A.A. Adam, Strength and durability properties of alkali activated slag and fly ash-based geopolymer concrete, School of Civil, Environmental and Chemical Engineering, RMIT University, Melbourne, Australia, 2009.
[33] A.M. Neville, Properties of Concrete, Fourth and Final ed., Standards updated to 2002, Pearson Education Limited, Harlow, 1996.
[34] AS, Method of testing concrete, Method 9: Determination of the compressive strength of concrete specimens, in: AS (Australian Standards), Standards Australia, Australia, 1999, pp. 1–12.
[35] AS, Methods of testing concrete – Determination of the modulus of rupture, in: AS (Australian Standards), Standards Australia, Australia, 2000, pp. 1–5.
[36] AS, Methods of testing concrete – Determination of indirect tensile strength of concrete cylinders (Brasil or splitting test), in: AS (Australian Standards), Standards Australia, Australia, 2000, pp. 1–5.
[37] AS, Methods of testing concrete – Determination of the static chord modulus of elasticity and Poisson's ratio of concrete specimens, in: AS (Australian Standards), Standards Australia, Australia, 1997.
[38] AS, Methods of testing concrete – Determination of mass per unit volume of hardened concrete – Water displacement method, in: AS (Australian Standards), Standards Australia, Australia, 1998.
[39] ASTM, Standard Test Method for Pulse Velocity Through Concrete, West Conshohocken, West Conshohocken, USA, 2009.
[40] AS, Methods of testing concrete – Determination of water absorption and apparent volume of permeable voids in hardened concrete. 1999, Standards Australia.
[41] AS, Concrete structures, in: AS (Australian Standards), Standards Australia, Australia, 2009, pp. 1–208.
[42] T. Bakharev, Geopolymeric materials prepared using Class F fly ash and elevated temperature curing, Cem. Concr. Res. 35 (6) (2005) 1224–1232.
[43] A. Palomo, M.W. Grutzeck, M.T. Blanco, Alkali-activated fly ashes: a cement for the future, Cem. Concr. Res. 29 (8) (1999) 1323–1329.
[44] F. Rendell, R. Jauberthie, M. Grantham, Deteriorated Concrete: Inspection and Physicochemical Analysis, Thomas Telford, 2002.
[45] VicRoads, Test Methods for the Assessment of Durability of Concrete, VicRoads, Australia, 2007.
[46] P. Basheer, F. Montgomery, A. Long, Clam'tests for measuring in situ permeation properties of concrete, Nondestr. Testing Eval. 12 (1) (1995) 53–73.
[47] A.P. System, Operating manual, S.o.C.E. Structural Materials Research Group, The Queen's University of Belfast, Northern Ireland, U.K., Editor. 1995, Structural Materials Research Group, Queen's University of Belfast, U.K.
[48] S.P. Yap, U.J. Alengaram, M.Z. Jumaat, Enhancement of mechanical properties in polypropylene–and nylon–fibre reinforced oil palm shell concrete, Mater. Des. 49 (1) (2013) 1034–1041.
[49] A. Garbacz, E.J. Garboczi, Ultrasonic evaluation methods applicable to polymer concrete composites, US Department of Commerce, Technology Administration, National Institute of Standards and Technology, 2003.
[50] R. Browne, M. Geoghegan, A. Baker, Analysis of structural condition from durability results, Corros. Reinforcement Concr. Constr. (1983) 193–222.
[51] M. Steveson, K. Sagoe-Crentsil, Relationships between composition, structure and strength of inorganic polymers, J. Mater. Sci. 40 (16) (2005) 4247–4259.
[52] J. Davidovits, High-alkali cements for 21st century concretes, ACI Special Publ. 144 (1994) 383–398.
[53] P. Duxson et al., The effect of alkali and Si/Al ratio on the development of mechanical properties of metakaolin-based geopolymers, Colloids Surf., A 292 (1) (2007) 8–20.
[54] E.I. Diaz, E.N. Allouche, S. Eklund, Factors affecting the suitability of fly ash as source material for geopolymers, Fuel 89 (5) (2010) 992–996.
[55] E. Alvarez-Ayuso et al., Environmental, physical and structural characterisation of geopolymer matrixes synthesised from coal (co-)combustion fly ashes, J. Hazard. Mater. 154 (2008) 175–183.
[56] L. Weng, K. Sagoe-Crentsil, Dissolution processes, hydrolysis and condensation reactions during geopolymer synthesis: Part I—Low Si/Al ratio systems, J. Mater. Sci. 42 (9) (2007) 2997–3006.
[57] C. Gunasekara et al., Zeta potential, gel formation and compressive strength of low calcium fly ash geopolymers, Constr. Build. Mater. 95 (1) (2015) 592–599.
[58] C. Tennakoon et al., Distribution of oxides in fly ash controls strength evolution of geopolymers, Constr. Build. Mater. 71 (2014) 72–82.